Published in final edited form as:
J Proteome Res. 2010 February 5; 9(2): 885. doi:10.1021/pr900784c.

Quantitative organellar proteomics analysis of rough endoplasmic reticulum from normal and acute pancreatitis rat pancreas

Xuequn Chen[1,*], **Maria Dolors Sans**[1], **John R. Strahler**[2], **Alla Karnovsky**[6], **Stephen A. Ernst**[4], **George Michailidis**[5,6], **Philip C. Andrews**[2,3,6], and **John A. Williams**[1,6]

[1]Department of Molecular & Integrative Physiology, The University of Michigan, Ann Arbor, MI

[2]Department of Biological Chemistry, The University of Michigan, Ann Arbor, MI

[3]Department of Chemistry, The University of Michigan, Ann Arbor, MI

[4]Department of Cell and Development Biology, The University of Michigan, Ann Arbor, MI

[5]Department of Statistics, The University of Michigan, Ann Arbor, MI

[6]Center for Computational Medicine and Bioinformatics, The University of Michigan, Ann Arbor, MI

Summary

The rough endoplasmic reticulum (RER) is a central organelle for synthesizing and processing digestive enzymes and alteration of ER functions may participate in the pathogenesis of acute pancreatitis (AP). To comprehensively characterize the normal and diseased RER subproteome, this study quantitatively compared the protein compositions of pancreatic RER between normal and AP animals using isobaric tags (iTRAQ) and 2D LC-MALDI-MS/MS. A total of 469 unique proteins were revealed from four independent experiments using two different AP models. These proteins belong to a large number of functional categories including ribosomal proteins, translocon subunits, chaperones, secretory proteins, and glyco- and lipid-processing enzymes. 37 RER proteins (25 unique in arginine-induced, 6 unique in caerulein-induced and 6 common in both models of AP) showed significant changes during AP including translational regulators and digestive enzymes whereas only mild changes were found in some ER chaperones. The six proteins common to both AP models including a decrease in pancreatic triacylglycerol lipase precursor, Erp27, and prolyl 4-hydroxylase beta polypeptide as well as a dramatic increase in fibrinogen alpha, beta and gamma chains. These results suggest that the early stages of AP involve changes of multiple RER proteins that may affect the synthesis and processing of digestive enzymes.

Keywords

Pancreas; Acute pancreatitis; Rough endoplasmic reticulum; iTRAQ; Organellar proteomics; Quantitative proteomics

* Corresponding author: Xuequn Chen, Department of Molecular & Integrative Physiology, 7703 Medical Science Building II, The University of Michigan, Ann Arbor, MI 48109, Tel.:734-7649456, Fax: 734-9368813, xuequnc@umich.edu.

Supporting Information Available: three supplemental tables containing all identified pancreatic RER proteins and their quantifications between normal and pancreatitis as well as a figure with higher magnification of immunocytochemistry results are available free of charge via the Internet at http://pubs.acs.org.

Introduction

Acute pancreatitis (AP) is a common clinical condition with a high morbidity and significant mortality [1-3]. It is generally believed that AP is initiated within acinar cells [1]. However, the cellular mechanisms of AP are not fully understood. In order to elucidate the initiating cellular events causing AP, several laboratory animal models mimicking human AP have been developed [4-9]. These models share several common features of the early stage disease including secretory blockade, edema, intracellular trypsin activation, high levels of digestive enzymes in blood, cytoplasmic vacuolization, activation of NFκB followed by the induction of an inflammatory response [10-13]. One of the most common models of AP is induced in rodents by administration of the cholecystokinin (CCK) analog caerulein in supermaximal physiological doses. This rapidly induces a relatively mild form of edematous pancreatitis [5]. By contrast, administration of a large amount of the amino acid arginine by intraperitoneal injection induces a slower but more severe, necrotizing pancreatitis [8, 14, 15]. The use of these models has advanced our understanding of the early cellular events that underlie the development of acute pancreatitis [16]. However, there is still no specific answer for a common triggering mechanism of the disease, especially at the subcellular level.

Pancreatic acinar cells are highly specialized for digestive enzyme synthesis, storage, and secretion [17], therefore they have abundant endoplasmic reticulum (ER) to meet the protein synthesis rate, the highest among all adult human tissues [18-21]. Disruption of ER homeostasis can cause ER stress which has been found to play critical roles in a number of diseases states, such as diabetes mellitus and Alzheimer disease [22, 23]. More importantly, it has been indicated that ER stress accompanied acute pancreatitis [24, 25] with the activation of major ER stress markers detected in the arginine model of experimental AP [25]. In addition, an earlier study showed the inhibition of global protein synthesis, predominantly digestive enzymes synthesis, during caerulein-induced pancreatitis in mice [26]. Due to the accumulating evidence, ER has become a reasonable target organelle for studying the intracellular triggering mechanism of AP. In this study, we conducted the first organellar proteomics study of pancreatic RER in normal and AP rats. The quantitative comparison was focused on isolated RER in order to enrich for the protein machinery involved in protein synthesis and protein folding. We wanted to test whether alteration of the protein composition of the RER could participate in the initiating cellular events during early AP.

Organellar proteomics represents an analytical strategy that combines biochemical fractionation and comprehensive protein identification [27]. Initial purification of organelles leads to reduced sample complexity and links proteomics data to functional analysis. Because of its central role in the secretory pathway, the ER has been the subject of several recent organellar proteomics studies [28, 29]. Using a bioinformatics approach, a human ER protein data base termed “Hera” has also been established which contained 499 human ER proteins [30]. In spite of the above comprehensive analyses for ER protein profiling, most of the proteomics studies to date have been focused on a single tissue source, the liver. Since tissue specific differences of organellar protein composition have been demonstrated in recent large scale comparative proteomics studies of mitochondria [29, 31], a comprehensive analysis of ER protein composition in other tissues such as pancreas is expected to provide additional insight into ER functions.

Recently, organellar proteomics has become more quantitative [32]. Among the quantitative proteomics approaches, iTRAQ is one of the recently developed chemical labeling reagents [33]. The commonly used version of iTRAQ reagent contains four isobaric tags and the most recent version of iTRAQ reagent contains eight tags. Therefore the tryptic peptides from up to eight different samples can be simultaneously quantified [34]. Quantitative proteomics analyses have been performed comparing total tissue proteins between normal pancreas and chronic

pancreatitis or pancreatic adenocarcinoma samples [35, 36]. However, very few studies have been applied to acute pancreatitis of animal models using whole pancreas tissue extract [37]. To our knowledge, no proteomics study focusing on subcellular organelles in animals of acute pancreatitis has been reported. In the current study, we applied organellar proteomics approaches to the analysis of the RER of the pancreas from normal and acute pancreatitis rats. A set of 469 pancreatic RER proteins is reported in this study among which a significant number showed changes in two different models of acute pancreatitis.

Methods

Reagents and Materials

Sequencing grade modified trypsin was from Promega (Madison, WI, USA). iTRAQ™ reagents were from Applied Biosystems (Foster City, CA). Caerulein and α-cyano-4-hydroxycinamic acid and other reagents were obtained from Sigma Chemical (St. Louis, MO, USA). SCX MicroSpin™ columns were from The Nest Group, Inc. (Southborough, MA). Zorbax C_{18} reversed-phase cartridge and Zorbax 300 SB C18 reversed-phase analytical column were purchased from Agilent (Palo Alto, CA). HPLC grade water and acetonitrile were purchased from Fisher Scientific (Pittsburgh, PA). All chemicals were of analytical grade and used as received. A number of antibodies were used in this study: anti-amylase from Sigma Chemicals, anti-chymotrypsin from Cortex (San Leandro, CA), anti-fibrinogen alpha and beta chains from Santa Cruz (Santa Cruz, CA), anti-BiP, anti-eEF1a1, anti-calreticulin, anti-VDAC 1 were from Abcam (Cambridge, MA), anti-S6 from Cell Signaling (Danvers, MA) and anti-cyclophilin A from Millipore (Temecula, CA).

Induction of Pancreatitis

Male Wistar rats (Harlan, Indianapolis, IN), 150-200 g were used in this study. To induce acute pancreatitis with arginine, rats were fasted overnight with *ad libitum* access to water and administered 4.0 g/kg body weight $_{L}$-arginine by i.p. injection in saline (pH 4.0) after which food and water were available *ad libitum*. Control animals followed the same experimental timing pattern but were injected with saline. Rats were euthanized in a CO_2 chamber, blood obtained by cardiac puncture and pancreas samples for cell fractionation were collected 24 h after arginine administration. To induce pancreatitis with caerulein, rats were injected i.p. with 3 hourly injections of 50 μg/kg synthetic caerulein dissolved in saline. Control animals followed the same experimental timing pattern but were injected with saline. Blood and pancreas were collected from control and caerulein-injected rats 6 hours after the first injection. To evaluate earlier time points, tissue was taken 30 min after a single injection or after 3 hourly injections. In each experimental group four to six animals were used to yield adequate statistical power based on power analysis of our previous experiments. Pancreatitis was characterized by biochemical and morphological criteria similar to our previous work.

Measurement of parameters for evaluating acute pancreatitis

Trypsin activity assay—Intracellular trypsin activity in pancreatic acinar cells was measured fluorimetrically using Boc-Gln-Ala-Arg-MCA as the substrate according to the method of Kawabata et al. [38]. The trypsin activity in the samples was calculated using a standard curve generated by assaying purified trypsin and expressed as ng of trypsin/mg of total protein.

Determination of pancreatic water content (edema)—The water content of the pancreas was quantified by weighing the freshly harvested tissue (wet weight) and compared with the weight of the same sample after desiccation at 90° C for 48 h (dry weight). The results were calculated and expressed as a percentage (wet weight-dry weight/wet weight ×100).

Determination of plasma amylase—Blood was collected by cardiac puncture with heparinized needles after previous exposure of rats to CO_2. The blood was centrifuged at 7,500 × g for 15 min and plasma (supernatant) stored at −20° C until assayed for amylase activity. Amylase assay was performed using the Phadebas Amylase Reagent.

Histology—Upon collection of pancreas, a portion of the tissue was fixed in 4% formaldehyde and embedded in paraffin for morphological evaluation by Hematoxylin and Eosin staining. Microscopic images were taken and effects of treatments on pancreatic inflammation, acinar atrophy and vacuolization were evaluated.

Immunocytochemistry—Pancreas from normal and cerulein-induced pancreatitis rats were fixed for 2 h with 4% formaldehyde. Immunofluorescence localization of alpha- and beta-fibrinogen was performed with cryostat sections using previous described methods [39]. Fibrinogen antibodies were diluted 1:100 to 1:200. Digital images were collected with an Olympus BX-51 epifluorescence microscope.

Isolation of RER

Pancreatic RER were isolated by established cell fractionation techniques as previously described [40]. Each pancreas was homogenized in ice cold buffered isotonic sucrose: 300 mM sucrose containing 20 mM HEPES, pH 7.4, 1 mM $MgCl_2$ and protease inhibitors (PMSF, aprotinin, and leupeptin) by use of a glass-Teflon motor-driven homogenizer. The homogenate was first centrifuged at 600 × g for 10 min at 4°C and then 12,000 × g for 20 min to remove all cell debris, nuclei, ZG and mitochondria. To isolate RER the post mitochondrial supernatant was centrifuged at 150,000 × g for 1 hour in a Beckman Ultracentrifuge using a Ti70 rotor to obtain a total microsomal pellet which was then re-suspended in 1 ml of resuspension buffer (20 mM HEPES, 1.28 M sucrose). A discontinuous sucrose gradient was prepared containing from top to bottom: 6 ml 0.3 M sucrose, 1.5 ml 1.15 M sucrose, 0.5 ml 1.28 M sucrose with the total microsomes, 1.5 ml 1.35 M sucrose and 2 ml 2 M sucrose. The tubes were then centrifuged for 90 min at 180,000 × g in a SW41 swinging bucket rotor and the RER collected at the 1.35 to 2 M sucrose interface. Purified RER microsomes were obtained as a pellet. To remove ribosomes from RER in a nondestructive manner, the purified RER was suspended in sucrose with 1.0 M KCl and 1 mM puromycin for 60 min at room temperature followed by 30 min on ice after which the stripped membranes were collected by centrifugation. ER pellets were stored at -80°C until use. Purity of the RER preparation was assessed by Western blotting for known marker proteins of different organelles and by electron microscopy as described previously. This stripping procedure also helps remove other contaminant molecules.

In-solution digestion, iTRAQ™ Labeling and 2D LC-MALDI-MS/MS

For in-solution digestion, the ER pellets prepared from control and pancreatitis rats were solubilized on ice in 50 μl buffer containing 500 mM TEAB (triethyl ammonium bicarbonate), 8 M urea and 0.4% SDS. After removing insoluble materials, protein concentrations were determined using the Bio-Rad Bradford assay kit. 50 μg ER protein from each group was reduced and then cysteines were blocked as previously described [39, 41]. The protein solution was diluted four times with 0.5M TEAB containing 5 μg trypsin (Promega sequencing grade, 1:10 w/w) and incubated at 37 °C overnight. To quantitatively compare protein abundance in the control and pancreatitis rats, tryptic digests from each rat were labeled with iTRAQ reagents. 4-plex reagents were used in the single time point studies of arginine- and caerulein-induced pancreatitis, two tags for two control rats and the other two tags for two pancreatitis rats. For the time course study of caerulein-induced pancreatitis, 8-plexed iTRAQ reagents were used to label two animals at each time point at 0, 30 min, 3 and 6 hours. The labeling procedure was according to the protocol provided by the manufacturer [33]. The reaction was

stopped by diluting the mixture with 10 volumes of strong cation exchange (SCX) buffer containing 10 mM KH_2PO_4 and 15% acetonitrile with pH adjusted to 3.

As previously described [39, 41], the iTRAQ™ labeled peptide mixture (~100 μg) was separated by 2D liquid chromatography. In the first dimension, the peptide mixture was fractionated on a strong cation exchange MicroSpin™ column with sequential elution of bound peptides in eight salt steps of 50 μl of 10mM potassium phosphate buffer (pH 3.0) containing 20, 50, 75, 100, 125, 150, 200 and 500 mM NaCl. The eluate from each salt step was dried in a SpeedVac, reconstituted with forty microliters 0.1% TFA and then separated by reversed phase chromatography using a Zorbax 300 SB C18 column, 75 μm × 150 mm, 3.5 μm particles on an Agilent 1100 HPLC system at 300 nl/min fow rate with the following binary gradient: 0 min, 6.5% B; 9 min, 6.5% B; 12 min, 15% B; 92 min, 45% B; 97 min, 60% B; 102 min, 100% B; 104 min, 100% B; 105 min, 6.5% B; 115 min, 6.5% B. Solvent A was 0.1% TFA and solvent B was 90% acetonitrile and 0.1% TFA. Column effluent was mixed with MALDI matrix (2mg/ml α-cyano-4-hydroxycinnamic acid) through a 25 nl mixing tee and spotted on 192 well MALDI target plates which were later analyzed by tandem mass spectrometry. The matrix was delivered to the mixing tee by an external infusion pump at 800 nl/min. The MS and MS/MS spectra were acquired on an Applied Biosystems 4800 Proteomics Analyzer (TOF/TOF) (Applied Biosystems/MDX Sciex, Foster City, CA) in positive ion reflection mode. Each MALDI plate was calibrated on nine calibration wells using seven peptide standards (angiotension III, 931.5148 Da, angiotensin II, 1046.5418 Da, angiotensin I, 1296.6851 Da, substance P, 1347.7354 Da, bombesin, 1619.8223 Da, ACTH 18-39, 2465.1983 Da, ACTH 7-38, 3657.9289 Da) with a 20 ppm mass accuracy in the MS mode. Both MS and MS/MS data were then acquired in the sample wells using the instrument default calibration. Typical MS spectra were obtained with the minimum possible laser energy in order to maintain the best resolution. Single-stage MS spectra for the entire samples were collected first and in each sample well MS/MS spectra were acquired from the 12 most intense peaks above the signal to noise ratio threshold of 60.

Database search and statistic analysis of iTRAQ results

Protein identification and quantification for iTRAQ experiments was carried out in the ProteinPilot™ software v2.0 (Applied Biosystems; MDS-Sciex) using the Paragon™ algorithm [42]. This software interacts directly with the Oracle database in which the mass spectrometer stores its data, and submits monoisotopic peak lists in batch to a local instance of the search engine for protein identities. No additional peak list filtering was specified. Peak lists were generated by the mass spectrometer during data acquisition based on a specified signal to noise threshold (30 in this case). To estimate the false positive discovery rate of peptide identification, a target decoy database was generated by manually concatenating the forward and reverse sequences in IPI rat database (version 3.34, with 38873 of *Rattus norvegicus* proteins) and used in all database searches. All reported proteins were identified with 95% or greater confidence as determined by ProteinPilot™ Unused scores (≥1.3) with the corresponding false positive discovery rate below 1%. The Paragon™ algorithm in ProteinPilot software was used as the default search program with iTRAQ-labeled peptide as sample type, trypsin as the digestion agent, methyl methanethiosulfonate for cysteine modification and 4800 TOF/TOF as the instrument. The Peptide Summary results obtained from ProteinPilot v2.0 software were exported to Microsoft Excel.

The peak areas of the iTRAQ reporters in each peptide were used in the in-house statistical analysis to calculate ratios of pancreatitis vs. control, their standard errors and the corresponding p-values as previously described [43, 44]. First, in order to compensate for the minor differences in actual total protein labeled in each sample it was necessary to normalize the raw peak areas. This was accomplished by matching the quantiles of the distributions of

the 115, 116, and 117 measurements to the quantiles of the 114 measurements using a monotone piecewise linear function. After normalization, the four peak area measurements exhibit similar statistics (mean, variance, quartiles). For the analysis of protein abundance changes using iTRAQ, the organization of the data was modeled as previously described [44] to account for variability of the observed MS/MS measurements both at the MS/MS spectrum level and at the peptide level. The peak area measurements from control or AP samples (114 &116 and 115 &117) were averaged prior to calculating ratios of treatment vs. control. Outlying observations (2%) at the peptide level were excluded based on the concept of relative data depth. Then, the observed ratios were modeled on a $\log_2$ scale, to overcome the lack of symmetry around 1 of the original scale and then transformed back to normal scale. The hypothesis of interest is whether the relative abundance (ratio) of protein $R = 1.0$, versus the alternative hypothesis that $R \neq 1.0$. To incorporate biological significance in the testing procedure, we chose cut points for the null hypothesis as follows: $H0$: $0.75 \leq R \leq 1.50$, corresponding to a decrease/increase of at least 25% and 50% before a change is called statistically significant. Previous experimental validation has demonstrated that as low as 23% differential expression of proteins could be detected by Western immunoblotting [44].

For functional categorization of identified RER proteins, the RER protein list was uploaded into DAVID[45] (The **D**atabase for **A**nnotation, **V**isualization and **I**ntegrated **D**iscovery) functional annotation tool using gene symbols as the identifiers and all the *Rattus Norvegicus* proteins as the background to perform the functional categorization. The Gene Ontology chart from the annotation summary results was used as the starting point based on which a thorough manual curation of each individual protein by an expert in the pancreas field were conducted using RGD[46] (Rat Genome Database) as a reference knowledgebase.

Results

Induction of Pancreatitis using two different animal models

In the current study, acute pancreatitis was induced using two different animal models by bolus injection of arginine or hyperstimulation by caerulein as in our previous studies [14, 26]. Histology and several commonly used parameters including pancreatic water content (edema), serum amylase and active trypsin were monitored to evaluate the severity of pancreatitis. As shown in Fig. 1, arginine injection induced edema (Fig. 1A), intrapancreatic trypsin activation (Fig. 1C) but not an increase in serum amylase (Fig. 1B). Histological evaluation showed vacuolization starting at 8 hours (data not shown) and necrosis with loss of apical cytoplasmic structures at 24 hours (Fig. 2D) compared to control pancreas (Fig. 2A). Neutrophils were seen in extracellular space at 24 hours (Fig. 2D). The small or absent increase in plasma amylase has previously been ascribed to the cellular damage and loss of apical zymogen granules [14, 26].

Caerulein-induced pancreatitis is a well established and well studied model of acute pancreatitis [5, 6]. In this model we injected rats with up to 3 hourly doses of caerulein (50 μg/kg) and then collected plasma and pancreas at 30 min, 4 hours and 6 hours after the first injection. As shown in Fig. 1 these animals showed elevated pancreatic edema (Fig. 1A), serum amylase (Fig. 1B) and intrapancreas trypsin activation (Fig. 1C). Trypsin activity is expected to peak (4 hour in our experiments and similarly in previous studies) and then decrease due to auto-degradation process following the activation of trypsin. Trypsin activity levels are still significantly higher in AP rat pancreas than in control pancreas after 6 hours which is indicative of acute pancreatitis (Fig. 1C). On histological exam, compared to control (Fig. 2A) intra-acinar vacuolization appeared as early as 30 min in caerulein-injected rats (Fig. 2B) and it became prominent at 4 hours (Fig. 2C). Infiltration of neutrophils was seen in extracellular space at 4 hours.

Isolation and Characterization of RER from rat pancreas

In this study, we purified RER from rat pancreas using discontinuous sucrose gradient and ultracentrifugation. As illustrated in Fig. 3, pancreatic RER was isolated by standard cell fractionation techniques including sucrose gradient centrifugation to separate RER from smooth ER and other membranes due to the higher density of attached ribosomes [40]. In order to detect lower abundant proteins, ribosomes were released from RER preparations by re-suspending RER pellets in buffer containing 1.0 M KCl and 1 mM puromycin. This nondestructive procedure does not lyse vesicles or remove ER content protein but significantly reduce the level of ribosomal proteins. An electron micrograph of purified rat pancreas RER vesicles before and after stripping is shown in Fig. 4A indicating the substantial reduction of ribosomes on RER membrane. It can also be observed that the RER preparation is free of visible contaminant organelles such as mitochondria and nuclei. The purity of the isolated RER was also assessed by Western blotting for known ER marker proteins as well as markers for potential contaminating organelles (VDAC1 for mitochondria, calreticulin and BiP for RER, cyclophilin A for cytosol). WB results from a representative RER preparation are shown in Fig. 4B. Compared to total lysate, the RER preparation was highly enriched for calreticulin and BiP whereas it was essentially free of mitochondrial and cytosolic proteins. In addition, the high salt and puromycin based ribosomal removal was 80-90% efficient although some ribosomes remain as shown by Western blotting for ribosomal protein S6. All together, the above rigorous evaluations including electron microscopy (Fig. 4A) and Western blotting with ER and other organellar markers (Fig. 4B) have confirmed the high purity of the RER preparation.

Although the induction of acute pancreatitis in both animal models caused pancreatic edema and morphological changes in exocrine pancreas (Fig. 1 and 2), we were able to prepare the RER from AP pancreas using the same procedure as from normal pancreas. The overall band pattern in the sucrose gradient and the yield of RER band (Fig. 3) were similar between AP and normal pancreas.

Pancreas ER proteome

The validation of the purity of our RER preparation and the successful induction of acute pancreatitis set a solid foundation for the subsequent characterization of the RER subproteome in normal pancreas and the quantitative comparison of RER protein abundances between normal and pancreatitis animals. Next, we compared the protein abundance of isolated, ribosome-reduced RER in normal and two models of acute pancreatitis rat pancreas using the iTRAQ approach. Biological duplication of a 4-plex experiment (two controls, two pancreatitis rats at 24 hours) was conducted using the arginine-induced AP model. In these two biological replicates, over 2,500 and 3,500 MS/MS spectra were identified leading to identification of over 1,500 and 2,200 distinct peptides respectively. For the caerulein-induced AP model, one 4-plex experiment (1,700 spectra and over 800 distinct peptides identified) and one 8-plex time course experiment (3,500 spectra and 1,800 distinct peptides identified), sharing one common time point at 6 hours after first injection, have been conducted. Combining all four data sets collected in this study, a total of over 11,000 MS/MS spectra were identified which accounted for 469 unique proteins with ProteinPilot Unused score equal to or greater than 1.3 (Supplemental Table 1) corresponding to 95% confidence or higher. This represents the first comprehensive characterization of the pancreatic ER subproteome.

The identified proteins were categorized according to several core ER functions (Fig. 5). These categories include protein translation & translocation, protein folding/chaperone, membrane trafficking, cytoskeleton, transporter proteins/calcium store, oligosaccharide biosynthesis, lipid & sterol biosynthesis, secretory and zymogen granule membrane proteins and metabolism. In addition, there is a group of proteins in the “Unknown functions” category which do not have functional information available in the public database or literature and

includes many hypothetical proteins. As an indication of the high purity of the RER preparation in this study, only 8% of the proteins were from known contaminating organelles such as mitochondria and nuclei (Supplemental Table 1 and Fig. 5). Since the nuclear envelope is continuous with ER membrane, the presence of some nuclear proteins in our RER samples might be expected. The largest category of proteins in the list is ribosomal proteins which account for 21% of total proteins. Although puromycin treatment has been shown to dramatically reduce ribosomes on ER membrane (Fig. 4A and 4B), essentially all the ribosomal small and large subunit proteins (86 total) have been identified. This is likely due to the overwhelming abundance of ribosomal proteins in pancreatic RER.

Determining changes in the relative abundance of individual proteins during the course of acute pancreatitis

By quantitatively comparing pancreatitis RER samples with controls, thirty-seven proteins, 25 in arginine-induced AP, 6 in caerulein-induced AP and 6 common in both models, have been found to increase or decrease based on the following criteria: changed in at least one of the two experiments with a ratio (treatment vs. control) ≤ 0.75 or ≥ 1.50 and $p \leq 0.05$ (Table 1, Table 2 and Supplemental table 2). It is worth noting that 4 proteins (Hsd17b13, Erp29, Fkbp11 and Ssr1) in arginine-induced AP model and another 4 proteins (Pdia2, Amy2, Prss1 and Pdia3) in caerulein-induced AP model showed significant changes (Supplemental table 2) with their mean ratios (treatment vs. control) meeting the above criteria. However, when considering their standard errors, their ratios could fall between 0.75 and 1.50. For this reason, they were not included in Table 1 and 2. In arginine AP, almost all the digestive enzymes showed dramatic reduction (decreased 50% to over 80%) and this was fully reproduced in duplicate experiments (Table 1). Compared to the large decrease of digestive enzymes, several ER chaperone proteins including 78 kDa glucose regulated protein precursor (BiP), prolyl 4-hydroxylase beta polypeptide and ERp27 showed a relatively mild decrease (Table 1) while other ER chaperones including Erp29, GRP 98 and GRP 150 did not change. Among the proteins that showed increase in AP animals, there are several clusters of proteins having different functions (Table 1). One cluster involved in protein translation includes eukaryotic translation initiation factor 4A and elongation factor 1 alpha 1. Another cluster, having the greatest increase in AP, includes fibrinogen alpha, beta and gamma chains. In addition, four tubulin chains were found increased 2 fold or more in AP rats (Table 1). Compared to the significant changes in arginine AP, caerulein-induced AP showed similarities as well as differences (Table 2). Common features between these two different animal models include mild decrease of ER chaperones prolyl 4-hydroxylase beta polypeptide, Erp27 and digestive enzyme, pancreatic triacylglycerol lipase precursor, as well as substantial increases for fibrinogen alpha, beta and gamma chains. In contrast to arginine-induced AP, only a few digestive enzymes showed a mild decrease in caerulein-induced AP at the 6 hour time point. In addition, several proteins functioning in protein translocation including signal recognition particle receptor (Srpr) and translocon associated protein subunit gamma (Ssr3) showed slight decreases (Table 2) whereas no significant changes were detected in arginine-induced AP in either of the two experiments (Srpr: 0.94 ± 0.05, 0.72 ± 0.26; Ssr3: 1.05 ± 0.05, 0.47 ± 0.48). The differences of protein changes in two animal models indicate that in addition to their common features these two models may represent different molecular mechanism in AP pathogenesis which requires future investigation.

As an initial effort to elucidate more complete dynamics of the protein changes during the pathogenesis of acute pancreatitis, we conducted a time course study using 8-plex iTRAQ reagents in the caerulein-induced AP model. The time course included four time points each with 2 rats: time 0, an early time point at 30 min after injection, an intermediate time at 3 hours and a later time point at 6 hours which was also used to confirm the result of caerulein-induced AP in the 4-plexed iTRAQ study (Table 2). The results of significant changes are shown in

Supplemental Table 3 and two clusters of proteins with different time course patterns are also shown in Fig. 6. It can be seen that a group of peripheral ER membrane proteins including Tram 1, Rrbp1, Srpr and Sptbn 5 increased as early as 30 min and returned to control level or went down at later time points. Different from this pattern, another group of proteins including three chains of fibrinogen showed a delayed change, with no detectable changes at 30 min, a dramatic increase at 3 hours then a reduction in levels at 6 hours. Our initial time course study provided additional information about protein dynamic changes during the course of AP and this work will be actively followed up in the near future studies.

Validation of up- or down-regulated proteins

To validate the significant changes found in the iTRAQ-based quantitative proteomics analyses, Western blotting analyses were performed on pancreatic RER samples from two control and two AP rats using antibodies against a number of representative proteins. In arginine AP, two proteins, amylase and chymotrypsin, were selected to represent the digestive enzyme group. It can be seen in Fig. 7 that these two proteins were dramatically reduced in two separate acute pancreatitis animals when compared with those of controls. In contrast to digestive enzymes, eEF1a1 and fibrinogen beta, representing translational machinery and fibrinogen subunits respectively, showed dramatic increases during AP. BiP which represents ER chaperons had little change in AP samples compared with normal samples. In caerulein AP, fibrinogen beta also showed dramatic increase in pancreatitis samples whereas amylase had only mild decrease in AP samples (the densitometry ratios of the four bands of C1, C2, P1 and P2 for amylase are 1.00:1.13:0.88:0.89) (Fig. 7). All the proteins tested in the WB studies confirmed the findings in the iTRAQ-based quantitative proteomics results (Table 1 and 2).

In the current study, all three chains (alpha, beta and gamma) of fibrinogen were among the most increased proteins in both AP animal models and this observation has been confirmed by Western blotting analysis of fibrinogen beta chain (Fig. 7). The fact that all three chains of fibrinogen were found highly increased in pancreas during acute pancreatitis made it intriguing to investigate the origin of the fibrinogen in AP rat pancreas. To elucidate whether fibrinogen was synthesized in acinar cells or it could have infiltrated from the external environment, we quantified the amount of mRNA for Fibrinogen alpha, beta and gamma by qRT-PCR using liver samples as a positive control. The messages for all fibrinogen chains were readily detectable in liver and increased in liver during AP. In contrast, in both control and AP rat pancreas, levels of mRNA for fibrinogen alpha and gamma were below the limits of detection and the levels for fibrinogen beta were detectable but extremely low (CT > 35) and we also considered them nondetectable (data not shown). We concluded that the fibrinogen chains detected in proteomics studies were not likely synthesized in pancreas. Instead, they are likely the result of infiltration from blood. Consistent with this possibility, our immunocytochemistry results (Fig. 8 with a higher magnification view in Supplement Fig. 1) using anti-fibrinogen α and β antibodies clearly demonstrated that the immunofluorescence was low in normal pancreas (Fig. 8 A, E) whereas in AP rats, the signals were very strong and mainly in the areas near blood vessel and intercellular spaces surrounding acini (Fig. 8 C, G). In addition, staining for fibrinogen beta chain was clearly enhanced over the basal cytoplasm of acinar cells following pancreatitis. These observations are all consistent with the fact that fibrinogen is a major acute response protein involved in the inflammation of pancreas.

Discussion

The endoplasmic reticulum (ER) is a central subcellular organelle for protein and lipid synthesis as well as Ca^{2+} regulation and maintaining ER homeostasis is critical for cell survival. For better understanding of its function, the ER has been the subject of several recent organellar proteomics studies. An early study using a 2D gel approach identified 141 proteins from

purified mouse liver ER vesicles [47]. Two new members of the thioredoxin family, Erp19 and ERp46, were identified in that study. In a more recent study [48], a protein correlation profiling strategy was applied to map proteins to ten subcellular locations in mouse liver by quantitatively comparing fractions collected from continuous density gradient centrifugation. A total of 229 proteins were clustered together with known ER markers and therefore assigned as ER proteins. In another recent effort to quantitatively define the subcellular components of the secretory pathway using individually purified RER, smooth microsomes and Golgi, over 800 proteins were assigned uniquely to the ER [28]. Since all the above studies utilized mouse or rat liver as the source of organelles, the knowledge gained about ER subproteome has been limited to a single tissue origin. Large scale proteomics studies comparing organelles across multiple organs have indicated the presence and functional importance of tissue specific organellar proteins [29, 31].

In this study, we obtained the first extensive catalog of pancreatic RER proteins with very minor contamination from other organelles including mitochodria and nuclei. This extensive list includes a full coverage of the key functional categories of ER (Figure 5 and Supplement table 1). Among these proteins, the largest functional group accounting for about 30% of total identified proteins is related to protein synthesis and translocation into ER. These include the protein translational machinery, essentially all the ribosomal subunits and major translation initiation and elongation factors. It also includes the entire machinery responsible for translocation of newly synthesized protein to ER membrane or lumen: components of signal recognition particle (SRP) and its receptor subunits to bind nascent polypeptides; the heterotrimeric SEC61 complex, SEC62 and SEC63 to function as the translocase; signal sequence receptor subunits and SEC11 signal peptidases to bind and remove signal peptides in ER lumen. One of the key functions of ER is to maintain a subcellular environment critical to correct protein folding. Consistent with this important function of ER, a major category of proteins identified are ER chaperones playing essential roles in protein folding and quality control. These include eight members of protein disulfide isomerases as well as the ER chaperones calreticulin, calnexin, BiP and several heat shock proteins. Given the high protein synthesis rate in exocrine pancreas and the importance of these proteins in protein folding, it is not surprising that all of these proteins were among the most abundant proteins in identified RER proteins when the relative protein abundance was estimated by spectral counting approach[49]. Since all the secretory proteins need to traffic through the ER, as expected a group of secretory proteins were detected in the ER samples including all the digestive enzymes and major zymogen granule membrane proteins such as GP2 and syncollin. Other categories of identified proteins were involved in other important functions of the ER including membrane trafficking, calcium storage, oligosaccharide, lipid & sterol biosynthesis. Many of these identified proteins are reported in pancreatic RER for the first time. One example is hypoxia up-regulated 1 which was one of the most abundant proteins found on RER in our study (Supplemental table 1). This protein has first been identified in astrocytes [50] and more recently has been shown to be induced during hypoxia or ER stress [22].

In an effort to search for the potential tissue specific ER proteins, we compared our list of pancreatic RER proteins with published results of liver ER lists [28, 48]. Protein sequences from two supplemental tables in that paper, one with 832 proteins unique to ER (Supplemental table S5A) and the other with 405 proteins (shared between ER and COPI vesicle) were retrieved from the NCBI database using batch Entrez and blasted on our local server against our pancreatic RER protein sequences. 162 proteins in the pancreatic RER were found not present in the liver ER data set (Supplemental table 1). Not surprisingly, all the pancreatic secretory proteins including all digestive enzymes and zymogen granule membrane proteins are uniquely found in our data set which demonstrate the validity of our comparison. Our data set comprises a more comprehensive set of protein translational machinery including ribosomal proteins and translation initiation factors. This might be attributed to the higher protein synthesis rate of

exocrine pancreas. There are also tissue specific ER lipid modifying enzymes and chaperones in exocrine pancreas. Endoplasmic reticulum protein 27 is of particular interest because it has been found decreased dramatically in RER of both models of acute pancreatitis.

In order to unveil the cellular mechanisms responsible for the initiation, propagation and limitation of the inflammatory response in the early phase of acute pancreatitis, several systemic profiling studies have been carried out recently using established animal models for AP. Microarray analysis was utilized to identify genes commonly induced in rat pancreatic acinar cells within 1-4 h in two *in vivo* AP models, caerulein and intraductal taurocholate administration [51]. This strategy yielded 51 known genes representing a complex array of molecules as well as identifying EGR-1 and several other novel genes likely to be important in the development and severity of acute pancreatitis. In a previous proteomics study, a 2D gel electrophoresis and MS/MS analyses were performed to compare whole pancreatic tissue extracts following AP induced by caerulein with pancreas from healthy rats [37]. A total of 125 proteins were identified from both diseased and control samples on the 2D gel and 42 proteins or protein fragments were found to be differentially expressed in diseased pancreas representing potential pathobiological pathways involved in this disease. These included activated digestive enzymes, increased expression of various inflammatory markers and changes related to oxidative and cellular stress responses. Three ER proteins were present among the 42 proteins, elongation factor 1-γ (decrease), 40S ribosomal protein SA (decrease) and PDI A6 (probable PTM) [37].

In this study, we conducted the first organellar proteomics study of normal and AP RER. We found 37 proteins that showed significant changes in at least one of the two experiments with ratios (treatment vs. control) ≤ 0.75 or ≥ 1.50 and $p \leq 0.05$. This corresponds to an 11% change out of the 320 proteins with 2 or more unique peptides. This is significantly above the 5% chance to detect a random change. Furthermore, many of the 37 proteins showed similar changes in duplicate experiments and a number of them were further validated by Western blotting and immunocytochemistry. The quantitative comparison was focused on isolated RER in order to enrich for the protein machinery involved in protein synthesis and protein folding. We wanted to test whether alteration of protein synthesis and induction of ER stress are initiating cellular events during early AP. Endoplasmic reticulum (ER) stress mechanisms have been found to play critical roles in a number of diseases, such as diabetes mellitus and Alzheimer's disease, but whether they are involved in acute pancreatitis is still uncertain. It has been shown that major ER stress sensing and signaling proteins including PERK, eIF2α, ATF6 and BiP are present in pancreatic exocrine acini and were activated early in the arginine model of experimental AP. For example, BiP was reported up-regulated within 4 h of injection of arginine and remained elevated for 24 hours [25]. We found BiP had little change in one experiment and decreased slightly in another experiment in the arginine AP model (Table 1). These observations do not support the induction of this compensatory mechanism in AP at least not in this model of pancreatitis. In terms of the other ER stress indicators such as PERK and ATF6, they were not identified with required confidence (95%) in our RER samples nor have been reported in other published proteomics studies [28, 48]. This is likely due to their very low abundance on the ER membrane. The decrease in digestive enzymes in the ER however, could be the result of the inhibition of their translation by PERK and exit from the RER as part of their maturation. An earlier study showed inhibition of global pancreatic protein synthesis during caerulein-induced pancreatitis in mice [26]. It is worth noting that Erp27, a non-catalytic ER-located protein disulfide isomerase family member [52], was found decreased in both animal models of acute pancreatitis. The exact function of this recently discovered protein in exocrine pancreas as well as its role in AP is not clear and is worth further investigation.

Translation initiation and elongation factors are proteins necessary for the regulation of protein synthesis in cells. Some of them play an important role in the association or dissociation of the

ribosomal subunits for the translation of the mRNA into protein and can be involved in cell stress mechanisms [53]. Others, as is the case for the eukaryotic initiation factor 4A (eIF4A), can be part of a functional subunit, the eukaryotic initiation factor 4F (eIF4F) complex, that recruits and unwinds the mRNA with an RNA-dependent ATPase activity. eIF4A is the most abundant initiation factor in cells and it has been shown to be involved with and increased in the response to cell stress [54-56]. Elongation factors, such as eukaryotic elongation factors 1 and 2 (eEF1 and eEF2), regulate translation elongation steps. In particular, eEF1α forms the ternary complex (eEF1α*GTP*aa-tRNA) which is then bound to the ribosomal A site in a codon-dependent manner. eEF1A has also been shown to be involved in cell stress [57, 58] and cancer processes [59]. In our studies these two translation factors, eEF1a1 and eIF4a1, increased in the RER after arginine pancreatitis, in correlation with the ER stress mechanisms that have already been demonstrated in this model of pancreatitis [25]. The fact that these molecules do not increase in the caerulein model is most likely related to the degree of cell damage which is less than that caused by arginine. Several other ER proteins, including the eukaryotic initiation factor 2α (eIF2α), the ER stress transducers PERK (PKR-like endoplasmic reticulum kinase), IRE1α (inositol requiring element-1α) and ATF6 (activating transcription factor 6), are expected to be phosphorylated rather than up-regulated in the ER stress response. Because this modification was not specifically targeted in our proteomics study of the ER, the potential changes of their phosphorylation were not observed. The reduction seen in the amount of ER chaperone molecules, such as BiP, ERp27, and P4hb in the development of arginine pancreatitis could be associated with the induction of apoptotic processes; the latest step in the ER stress and UPR (unfolded protein response) mechanisms, when chaperoning for unfolded proteins is no longer needed.

It has been demonstrated that during the induction of experimental models of acute pancreatitis the tubulin cytoskeleton is disrupted and degraded [60, 61]. In a proteome analysis of rat pancreatic acinar (AR42J) cells, tubulin β-chain was found to be differentially expressed [62] in caerulein-treated cells. In another study, the induction of two different models of acute pancreatitis to Balb/c and FVB/n mice, caused a slight increase of mRNA levels for tubulin in the pancreatitis groups [63]. In our study, the caerulein model of pancreatitis did not show any significant change in the amount of these tubulin isoforms in the ER. The arginine model, in contrast, exhibited an increase in several tubulin isoforms. Since the results (no change or decrease) found in the caerulein model are in concordance with what it has been found before in other studies [60, 61], we hypothesize that changes in the tubulin cytoskeleton of acinar cells are model-specific and indicative of differences in pathologies between the two models. It has been speculated that microtubules are most likely involved in the transport of zymogen granules from the Golgi to the apical pole of the cell and this process is disrupted during pancreatitis [61], but the role of microtubules in pancreatitis has not yet been fully determined. Thus, the differences between the caerulein and arginine models could likely be dependent upon the degree of cell damage in these two models of pancreatitis.

Fibrinogen, synthesized by the liver with little evidence for synthesis by other tissues, is the principal protein of vertebrate blood clotting containing two sets of three different chains (α, β, and γ) linked to each other by disulfide bonds. Inflammation and blood coagulation has been shown to be closely linked. The fact that fibrinogen is highly up-regulated in acute pancreatitis is consistent with it being a major acute response protein during the inflammation of pancreas. Our RT-PCR results indicated that fibrinogen was not synthesized within the pancreas. Whether or not the fibrinogen was absorbed into acinar cells via retrograde transport during inflammation is still an open question and requires further investigation. Interestingly, fibrinogen was found to be 3.0-fold up-regulated in human pancreatitic juice during pancreatitis compared with normal pancreatic juice in a proteomics study using ICAT reagent and LC-MS/MS [64].

In this study, we isolated highly purified pancreatic RER from normal and acute pancreatitis rats. Using iTRAQ-based quantitative proteomics approach, we reported the first comprehensive protein inventory of pancreatic RER which includes 469 proteins with a full coverage of core ER functional categories and minimal contaminating organellar proteins. Furthermore, we quantified RER protein changes during the early course of acute pancreatitis using two different animal models. Significant RER protein changes were found in multiple functional categories including translational regulator, digestive enzymes, chaperones and cytoskeleton proteins. These results suggested that the early stages of acute pancreatitis involve changes of multiple aspects of RER functions including the synthesis and processing of digestive enzymes.

Supplementary Material

Refer to Web version on PubMed Central for supplementary material.

Acknowledgments

We thank Nancy Vogel for assistance in Western blotting analysis and Brad Nelson for immunocytochemistry and electron microscopy. This research was supported by NIH grant R37 DK41122 to J.A.W., the National Resource for Proteomics and Pathways (P41 RR018627) to P.C.A. and the University of Michigan Gastrointestinal Peptide Center (P30 DK34933) whose Proteomics and Cell Biology and Cell Imaging Cores were utilized. Support was also received as a pilot grant from the Center for Computational Medicine and Bioinformatics at the University of Michigan.

References

1. Saluja AK, Lerch MM, Phillips PA, Dudeja V. Why does pancreatic overstimulation cause pancreatitis? Annu Rev Physiol 2007;69:249–69. [PubMed: 17059357]
2. Steer ML. Pathogenesis of acute pancreatitis. Digestion 1997;58:46–9. [PubMed: 9225091]
3. Adler G. Has the biology and treatment of pancreatic diseases evolved? Best Pract Res Clin Gastroenterol 2004;18:83–90. [PubMed: 15588799]
4. Bhatia M, Wong FL, Cao Y, Lau HY, Huang J, Puneet P, Chevali L. Pathophysiology of acute pancreatitis. Pancreatology 2005;5(23):132–44. [PubMed: 15849484]
5. Lampel M, Kern HF. Acute interstitial pancreatitis in the rat induced by excessive doses of a pancreatic secretagogue. Virchows Arch A Pathol Anat Histol 1977;373(2):97–117. [PubMed: 139754]
6. Niederau C, Ferrell LD, Grendell JH. Caerulein-induced acute necrotizing pancreatitis in mice: protective effects of proglumide, benzotript, and secretin. Gastroenterology 1985;88(5 Pt 1):1192–204. [PubMed: 2984080]
7. Lombardi B, Estes LW, Longnecker DS. Acute hemorrhagic pancreatitis (massive necrosis) with fat necrosis induced in mice by DL-ethionine fed with a choline-deficient diet. Am J Pathol 1975;79(3): 465–80. [PubMed: 1094837]
8. Tani S, Itoh H, Okabayashi Y, Nakamura T, Fujii M, Fujisawa T, Koide M, Otsuki M. New model of acute necrotizing pancreatitis induced by excessive doses of arginine in rats. Dig Dis Sci 1990;35(3): 367–74. [PubMed: 2307082]
9. Dawra R, Sharif R, Phillips P, Dudeja V, Dhaulakhandi D, Saluja AK. Development of a new mouse model of acute pancreatitis induced by administration of L-arginine. Am J Physiol Gastrointest Liver Physiol 2007;292(4):G1009–18. [PubMed: 17170029]
10. Grady T, Saluja A, Kaiser A, Steer M. Edema and intrapancreatic trypsinogen activation precede glutathione depletion during caerulein pancreatitis. Am J Physiol 1996;271(1 Pt 1):G20–6. [PubMed: 8760102]
11. Hofbauer B, Saluja AK, Lerch MM, Bhagat L, Bhatia M, Lee HS, Frossard JL, Adler G, Steer ML. Intra-acinar cell activation of trypsinogen during caerulein-induced pancreatitis in rats. Am J Physiol 1998;275(2 Pt 1):G352–62. [PubMed: 9688663]
12. Steinle AU, Weidenbach H, Wagner M, Adler G, Schmid RM. NF-kappaB/Rel activation in cerulein pancreatitis. Gastroenterology 1999;116(2):420–30. [PubMed: 9922324]

13. Chen X, Ji B, Han B, Ernst SA, Simeone D, Logsdon CD. NF-kappaB activation in pancreas induces pancreatic and systemic inflammatory response. Gastroenterology 2002;122(2):448–57. [PubMed: 11832459]

14. Tashiro M, Schafer C, Yao H, Ernst SA, Williams JA. Arginine induced acute pancreatitis alters the actin cytoskeleton and increases heat shock protein expression in rat pancreatic acinar cells. Gut 2001;49(2):241–50. [PubMed: 11454802]

15. Mizunuma T, Kawamura S, Kishino Y. Effects of injecting excess arginine on rat pancreas. J Nutr 1984;114(3):467–71. [PubMed: 6199486]

16. Pandol SJ, Saluja AK, Imrie CW, Banks PA. Acute pancreatitis: bench to the bedside. Gastroenterology 2007;132(3):1127–51. [PubMed: 17383433]

17. Williams JA. Intracellular signaling mechanisms activated by cholecystokinin-regulating synthesis and secretion of digestive enzymes in pancreatic acinar cells. Annu Rev Physiol 2001;63:77–97. [PubMed: 11181949]

18. Case RM. Synthesis, intracellular transport and discharge of exportable proteins in the pancreatic acinar cell and other cells. Biol Rev Camb Philos Soc 1978;53(2):211–354. [PubMed: 208670]

19. Jamieson JD, Palade GE. Intracellular transport of secretory proteins in the pancreatic exocrine cell. 3. Dissociation of intracellular transport from protein synthesis. J Cell Biol 1968;39(3):580–8. [PubMed: 5699932]

20. Jamieson JD, Palade GE. Intracellular transport of secretory proteins in the pancreatic exocrine cell. II. Transport to condensing vacuoles and zymogen granules. J Cell Biol 1967;34(2):597–615. [PubMed: 6035648]

21. Jamieson JD, Palade GE. Intracellular transport of secretory proteins in the pancreatic exocrine cell. I. Role of the peripheral elements of the Golgi complex. J Cell Biol 1967;34(2):577–96. [PubMed: 6035647]

22. Malhotra JD, Kaufman RJ. Endoplasmic reticulum stress and oxidative stress: a vicious cycle or a double-edged sword? Antioxid Redox Signal 2007;9(12):2277–93. [PubMed: 17979528]

23. Marciniak SJ, Ron D. Endoplasmic reticulum stress signaling in disease. Physiol Rev 2006;86(4): 1133–49. [PubMed: 17015486]

24. Kowalik AS, Johnson CL, Chadi SA, Weston JY, Fazio EN, Pin CL. Mice lacking the transcription factor Mist1 exhibit an altered stress response and increased sensitivity to caerulein-induced pancreatitis. Am J Physiol Gastrointest Liver Physiol 2007;292(4):G1123–32. [PubMed: 17170023]

25. Kubisch CH, Sans MD, Arumugam T, Ernst SA, Williams JA, Logsdon CD. Early activation of endoplasmic reticulum stress is associated with arginine-induced acute pancreatitis. Am J Physiol Gastrointest Liver Physiol 2006;291(2):G238–45. [PubMed: 16574987]

26. Sans MD, DiMagno MJ, D'Alecy LG, Williams JA. Caerulein-induced acute pancreatitis inhibits protein synthesis through effects on eIF2B and eIF4F. Am J Physiol Gastrointest Liver Physiol 2003;285(3):G517–28. [PubMed: 12773302]

27. Yates JR 3rd, Gilchrist A, Howell KE, Bergeron JJ. Proteomics of organelles and large cellular structures. Nat Rev Mol Cell Biol 2005;6(9):702–14. [PubMed: 16231421]

28. Gilchrist A, Au CE, Hiding J, Bell AW, Fernandez-Rodriguez J, Lesimple S, Nagaya H, Roy L, Gosline SJ, Hallett M, Paiement J, Kearney RE, Nilsson T, Bergeron JJ. Quantitative proteomics analysis of the secretory pathway. Cell 2006;127(6):1265–81. [PubMed: 17174899]

29. Kislinger T, Cox B, Kannan A, Chung C, Hu P, Ignatchenko A, Scott MS, Gramolini AO, Morris Q, Hallett MT, Rossant J, Hughes TR, Frey B, Emili A. Global survey of organ and organelle protein expression in mouse: combined proteomic and transcriptomic profiling. Cell 2006;125(1):173–86. [PubMed: 16615898]

30. Scott M, Lu G, Hallett M, Thomas DY. The Hera database and its use in the characterization of endoplasmic reticulum proteins. Bioinformatics 2004;20(6):937–44. [PubMed: 14751973]

31. Mootha VK, Bunkenborg J, Olsen JV, Hjerrild M, Wisniewski JR, Stahl E, Bolouri MS, Ray HN, Sihag S, Kamal M, Patterson N, Lander ES, Mann M. Integrated analysis of protein composition, tissue diversity, and gene regulation in mouse mitochondria. Cell 2003;115(5):629–40. [PubMed: 14651853]

32. Andersen JS, Mann M. Organellar proteomics: turning inventories into insights. EMBO Rep 2006;7 (9):874–9. [PubMed: 16953200]

33. Ross PL, Huang YN, Marchese JN, Williamson B, Parker K, Hattan S, Khainovski N, Pillai S, Dey S, Daniels S, Purkayastha S, Juhasz P, Martin S, Bartlet-Jones M, He F, Jacobson A, Pappin DJ. Multiplexed protein quantitation in saccharomyces cerevisiae using amine-reactive isobaric tagging reagents. Mol Cell Proteomics 2004;3(12):1154–69. [PubMed: 15385600]
34. Ow SY, Cardona T, Taton A, Magnuson A, Lindblad P, Stensjo K, Wright PC. Quantitative shotgun proteomics of enriched heterocysts from Nostoc sp. PCC 7120 using 8-plex isobaric peptide tags. J Proteome Res 2008;7(4):1615–28. [PubMed: 18290607]
35. Chen R, Brentnall TA, Pan S, Cooke K, Moyes KW, Lane Z, Crispin DA, Goodlett DR, Aebersold R, Bronner MP. Quantitative proteomics analysis reveals that proteins differentially expressed in chronic pancreatitis are also frequently involved in pancreatic cancer. Mol Cell Proteomics 2007;6 (8):1331–42. [PubMed: 17496331]
36. Crnogorac-Jurcevic T, Gangeswaran R, Bhakta V, Capurso G, Lattimore S, Akada M, Sunamura M, Prime W, Campbell F, Brentnall TA, Costello E, Neoptolemos J, Lemoine NR. Proteomic analysis of chronic pancreatitis and pancreatic adenocarcinoma. Gastroenterology 2005;129(5):1454–63. [PubMed: 16285947]
37. Fetaud V, Frossard JL, Farina A, Pastor CM, Buhler L, Dumonceau JM, Hadengue A, Hochstrasser DF, Lescuyer P. Proteomic profiling in an animal model of acute pancreatitis. Proteomics 2008;8 (17):3621–31. [PubMed: 18686302]
38. Kawabata S, Miura T, Morita T, Kato H, Fujikawa K, Iwanaga S, Takada K, Kimura T, Sakakibara S. Highly sensitive peptide-4-methylcoumaryl-7-amide substrates for blood-clotting proteases and trypsin. Eur J Biochem 1988;172(1):17–25. [PubMed: 3278905]
39. Chen X, Walker AK, Strahler JR, Simon ES, Tomanicek-Volk SL, Nelson BB, Hurley MC, Ernst SA, Williams JA, Andrews PC. Organellar proteomics: analysis of pancreatic zymogen granule membranes. Mol Cell Proteomics 2006;5(2):306–12. [PubMed: 16278343]
40. Preissler M, Williams JA. Localization of ATP-dependent calcium transport activity in mouse pancreatic microsomes. J Membr Biol 1983;73(2):137–44. [PubMed: 6864771]
41. Chen X, Ulintz PJ, Simon ES, Williams JA, Andrews PC. Global topology analysis of pancreatic zymogen granule membrane proteins. Mol Cell Proteomics 2008;7(12):2323–36. [PubMed: 18682380]
42. Shilov IV, Seymour SL, Patel AA, Loboda A, Tang WH, Keating SP, Hunter CL, Nuwaysir LM, Schaeffer DA. The Paragon Algorithm, a next generation search engine that uses sequence temperature values and feature probabilities to identify peptides from tandem mass spectra. Mol Cell Proteomics 2007;6(9):1638–55. [PubMed: 17533153]
43. Keshamouni VG, Jagtap P, Michailidis G, Strahler JR, Kuick R, Reka AK, Papoulias P, Krishnapuram R, Srirangam A, Standiford TJ, Andrews PC, Omenn GS. Temporal quantitative proteomics by iTRAQ 2D-LC-MS/MS and corresponding mRNA expression analysis identify post-transcriptional modulation of actin-cytoskeleton regulators during TGF-beta-Induced epithelial-mesenchymal transition. J Proteome Res 2009;8(1):35–47. [PubMed: 19118450]
44. Keshamouni VG, Michailidis G, Grasso CS, Anthwal S, Strahler JR, Walker A, Arenberg DA, Reddy RC, Akulapalli S, Thannickal VJ, Standiford TJ, Andrews PC, Omenn GS. Differential protein expression profiling by iTRAQ-2DLC-MS/MS of lung cancer cells undergoing epithelial-mesenchymal transition reveals a migratory/invasive phenotype. J Proteome Res 2006;5(5):1143–54. [PubMed: 16674103]
45. Huang da W, Sherman BT, Tan Q, Kir J, Liu D, Bryant D, Guo Y, Stephens R, Baseler MW, Lane HC, Lempicki RA. DAVID Bioinformatics Resources: expanded annotation database and novel algorithms to better extract biology from large gene lists. Nucleic Acids Res 2007;35(Web Server issue):W169–75. [PubMed: 17576678]
46. Twigger SN, Shimoyama M, Bromberg S, Kwitek AE, Jacob HJ. The Rat Genome Database, update 2007--easing the path from disease to data and back again. Nucleic Acids Res 2007;35(Database issue):D658–62. [PubMed: 17151068]
47. Knoblach B, Keller BO, Groenendyk J, Aldred S, Zheng J, Lemire BD, Li L, Michalak M. ERp19 and ERp46, new members of the thioredoxin family of endoplasmic reticulum proteins. Mol Cell Proteomics 2003;2(10):1104–19. [PubMed: 12930873]
48. Foster LJ, de Hoog CL, Zhang Y, Xie X, Mootha VK, Mann M. A mammalian organelle map by protein correlation profiling. Cell 2006;125(1):187–99. [PubMed: 16615899]

49. Liu H, Sadygov RG, Yates JR 3rd. A model for random sampling and estimation of relative protein abundance in shotgun proteomics. Anal Chem 2004;76(14):4193–201. [PubMed: 15253663]
50. Lee WH, Wang GM, Seaman LB, Vannucci SJ. Coordinate IGF-I and IGFBP5 gene expression in perinatal rat brain after hypoxia-ischemia. J Cereb Blood Flow Metab 1996;16(2):227–36. [PubMed: 8594054]
51. Ji B, Chen XQ, Misek DE, Kuick R, Hanash S, Ernst S, Najarian R, Logsdon CD. Pancreatic gene expression during the initiation of acute pancreatitis: identification of EGR-1 as a key regulator. Physiol Genomics 2003;14(1):59–72. [PubMed: 12709512]
52. Alanen HI, Williamson RA, Howard MJ, Hatahet FS, Salo KE, Kauppila A, Kellokumpu S, Ruddock LW. ERp27, a new non-catalytic endoplasmic reticulum-located human protein disulfide isomerase family member, interacts with ERp57. J Biol Chem 2006;281(44):33727–38. [PubMed: 16940051]
53. Sans MD, Williams JA. Translational control of protein synthesis in pancreatic acinar cells. Int J Gastrointest Cancer 2002;31(13):107–15. [PubMed: 12622421]
54. Montero-Lomeli M, Morais BL, Figueiredo DL, Neto DC, Martins JR, Masuda CA. The initiation factor eIF4A is involved in the response to lithium stress in Saccharomyces cerevisiae. J Biol Chem 2002;277(24):21542–8. [PubMed: 11940596]
55. Lin JC, Hsu M, Tarn WY. Cell stress modulates the function of splicing regulatory protein RBM4 in translation control. Proc Natl Acad Sci U S A 2007;104(7):2235–40. [PubMed: 17284590]
56. Shen R, Weng C, Yu J, Xie T. eIF4A controls germline stem cell self-renewal by directly inhibiting BAM function in the Drosophila ovary. Proc Natl Acad Sci U S A. 2009
57. Chang R, Wang E. Mouse translation elongation factor eEF1A-2 interacts with Prdx-I to protect cells against apoptotic death induced by oxidative stress. J Cell Biochem 2007;100(2):267–78. [PubMed: 16888816]
58. Borradaile NM, Buhman KK, Listenberger LL, Magee CJ, Morimoto ET, Ory DS, Schaffer JE. A critical role for eukaryotic elongation factor 1A-1 in lipotoxic cell death. Mol Biol Cell 2006;17(2):770–8. [PubMed: 16319173]
59. Chen L, Madura K. Increased proteasome activity, ubiquitin-conjugating enzymes, and eEF1A translation factor detected in breast cancer tissue. Cancer Res 2005;65(13):5599–606. [PubMed: 15994932]
60. Jungermann J, Lerch MM, Weidenbach H, Lutz MP, Kruger B, Adler G. Disassembly of rat pancreatic acinar cell cytoskeleton during supramaximal secretagogue stimulation. Am J Physiol 1995;268(2 Pt 1):G328–38. [PubMed: 7864130]
61. Ueda T, Takeyama Y, Kaneda K, Adachi M, Ohyanagi H, Saitoh Y. Protective effect of a microtubule stabilizer taxol on caerulein-induced acute pancreatitis in rat. J Clin Invest 1992;89(1):234–43. [PubMed: 1370296]
62. Yu JH, Yun SY, Lim JW, Kim H, Kim KH. Proteome analysis of rat pancreatic acinar cells: implication for cerulein-induced acute pancreatitis. Proteomics 2003;3(12):2446–53. [PubMed: 14673795]
63. Zhong B, Omary MB. Actin overexpression parallels severity of pancreatic injury. Exp Cell Res 2004;299(2):404–14. [PubMed: 15350539]
64. Chen R, Pan S, Cooke K, Moyes KW, Bronner MP, Goodlett DR, Aebersold R, Brentnall TA. Comparison of pancreas juice proteins from cancer versus pancreatitis using quantitative proteomic analysis. Pancreas 2007;34(1):70–9. [PubMed: 17198186]

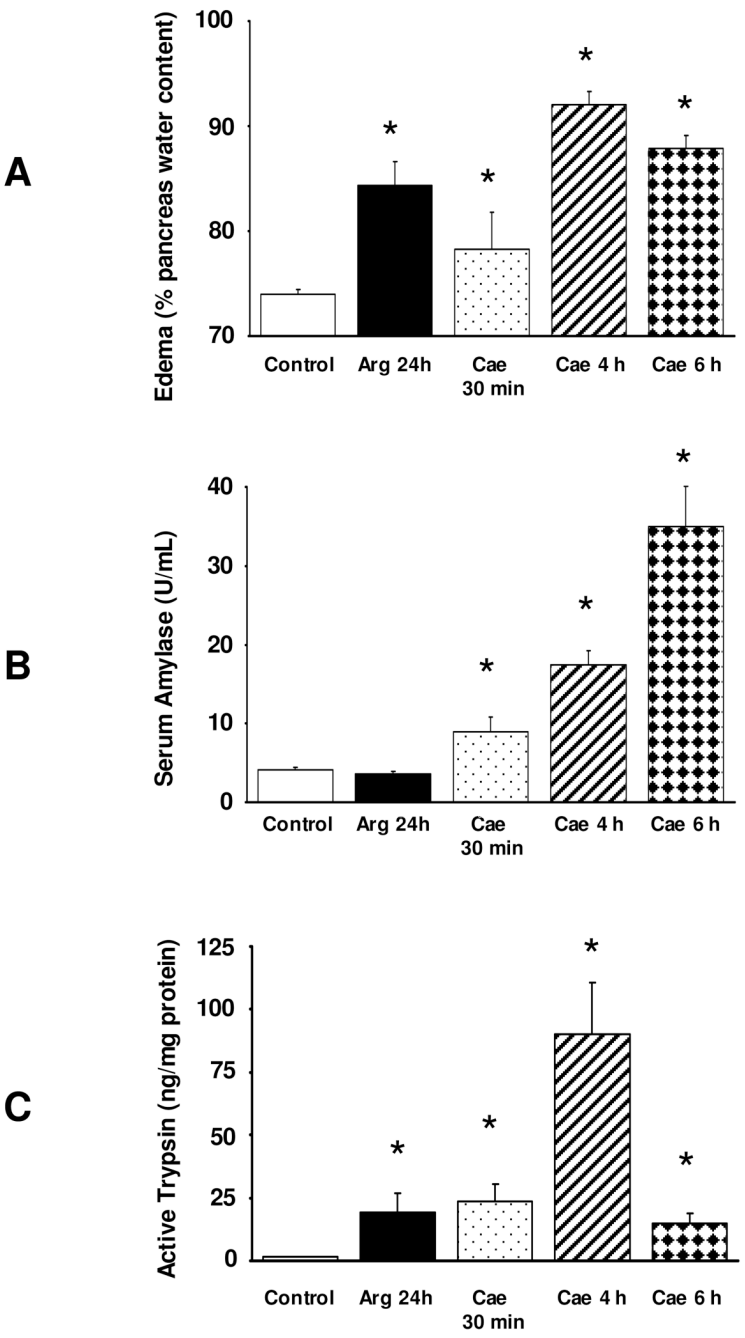

Figure 1. Acute pancreatitis parameters

Rats were treated with a single i.p. injection of L-arginine, or multiple i.p. injections of caerulein, or saline as indicated in the Material and Methods section; pancreas samples were collected at different times after acute pancreatitis induction. The groups were as follows: Control (average of control groups for caerulein and arginine pancreatitis); Arg 24 h (pancreas collected 24 h after arginine (4g/Kg) injection); Cae 30 min (pancreas collected 30 min after one single dose of 50 μg/Kg caerulein); Cae 4 h and Cae 6 h (pancreas collected 4 and 6 h after the first injection of a total of three hourly injections of 50 μg/Kg caerulein). Graphic representation of Edema (% of water content) in the pancreas (**A**), serum amylase levels (as

U/mL) (**B**) and (**C**) pancreatic active trypsin (as ng of trypsin/mg of protein). Results shown are means ± SE, * $p<0.05$; n=6-12.

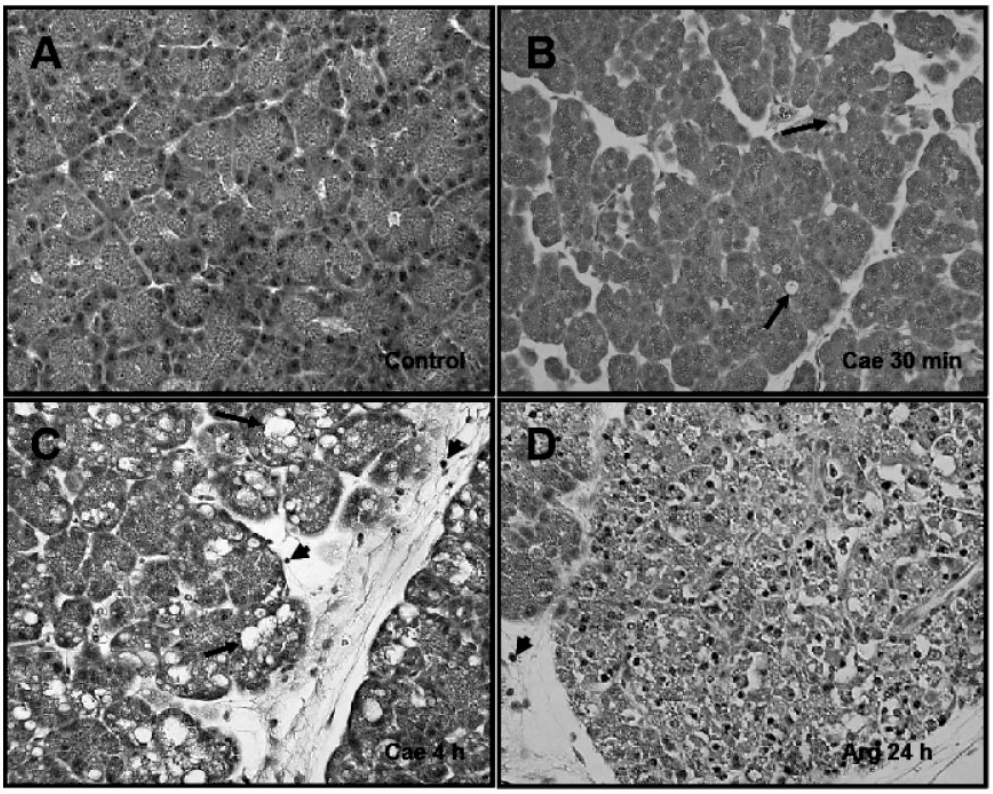

Figure 2. Histology of rat pancreas in normal and acute pancreatitis rats

A. Normal rat pancreas; B. 30 min after injection of caerulein; C. 4 hours after the first injection of caerulein; D. 24 hours after the injection of arginine. *Arrows* point to intracellular vacuoles and *arrowheads* to neutrophil infiltrations.

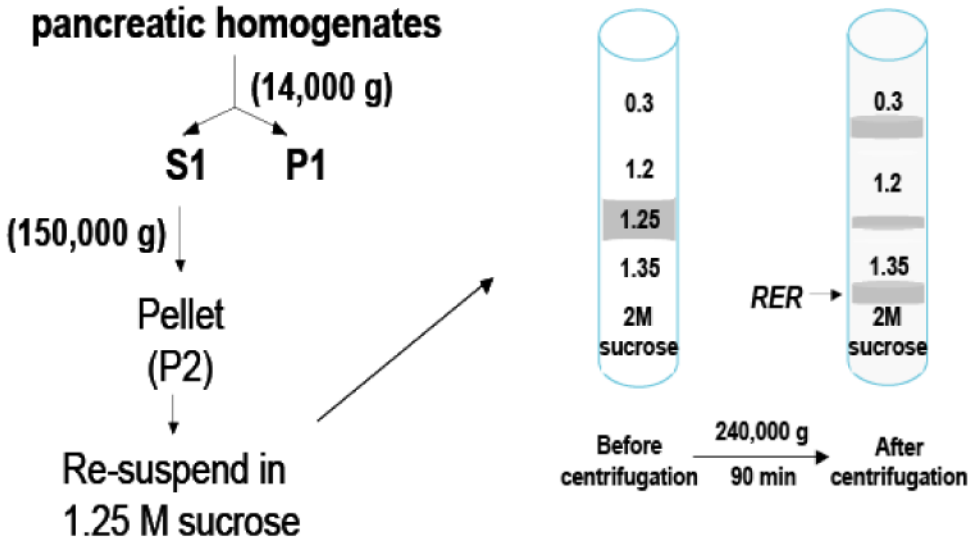

Figure 3. Workflow of RER purification from rat pancreas

Rat pancreas was first homogenized and after two centrifugations, the total microsome pellet was re-suspended in 1.25 M sucrose. A discontinuous sucrose gradient was prepared with the re-suspended microsome in the middle. After a 90 min ultracentrifugation at 240,000 g, RER was collected from the bottom band at the interface between 1.35 M and 2 M sucrose.

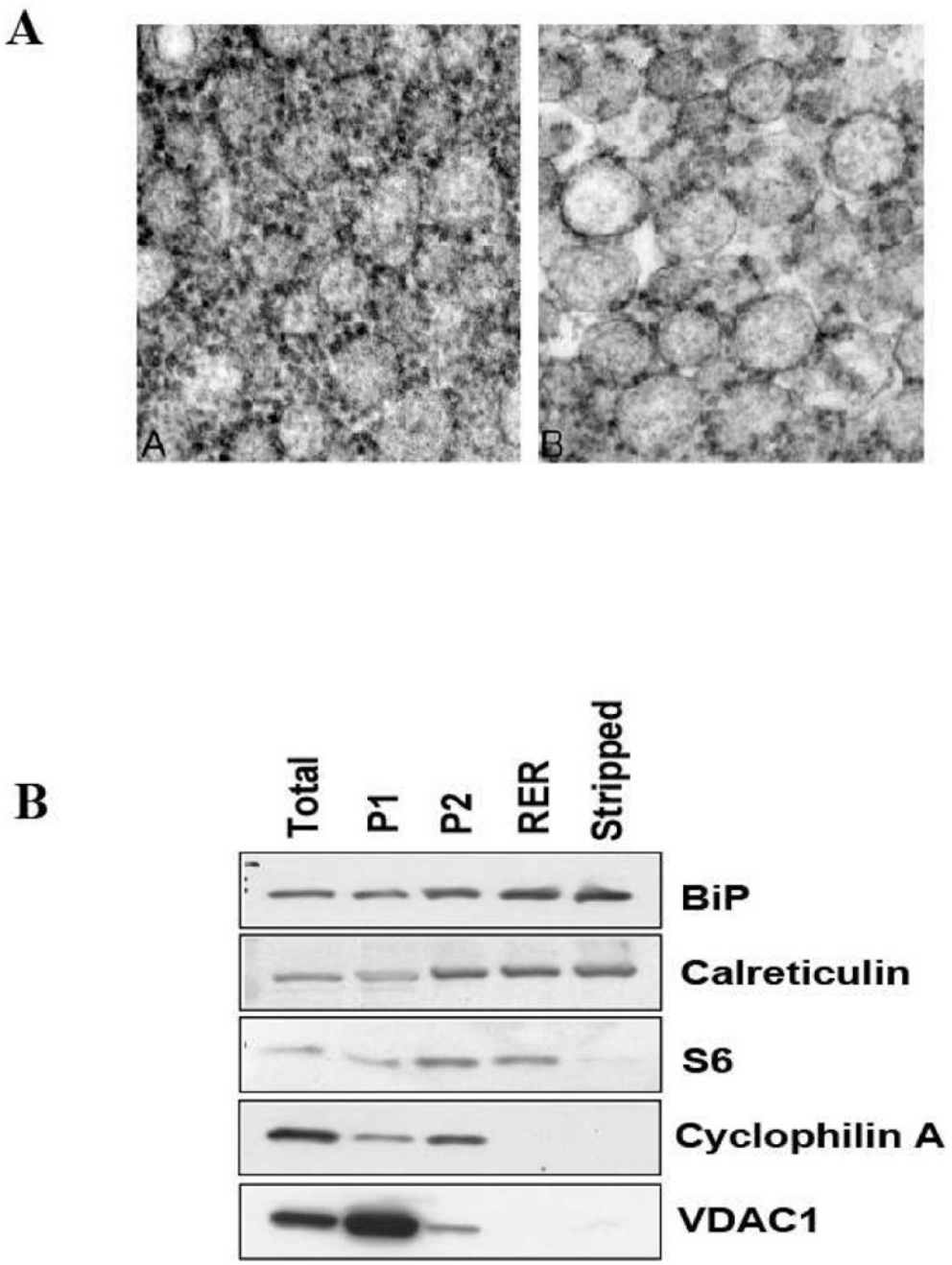

Figure 4. Examination of the purity of the pancreatic RER preparation

A. electron micrographs of RER prepared from rat pancreas (panel A, Left) and after subjecting to puromycin, high salt treatment to remove ribosomes (panel B, Right). B. Western blots of selected proteins in pancreatic lysate (total), a 14,000 g pellet (P1), a subsequent 150,000 g pellet (P2), RER purified on a sucrose gradient and RER stripped with puromycin and high salt. Note the enrichment of RER proteins and lack of cytoplasmic and mitochondrial marker proteins in the final stripped RER.

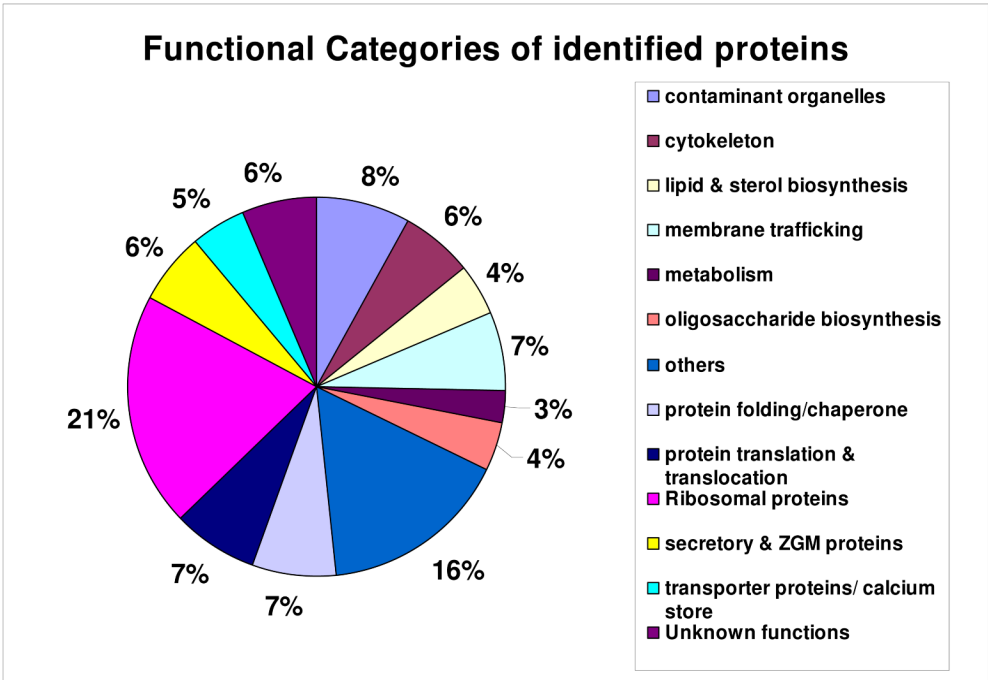

Figure 5. Functional classification of the pancreatic RER proteins

469 identified RER proteins were classified in 13 categories based on their functions. The percentage of total proteins in each category is illustrated in the pie chart. All the categories are listed on the side of the pie-chart each of which is coded with a different color.

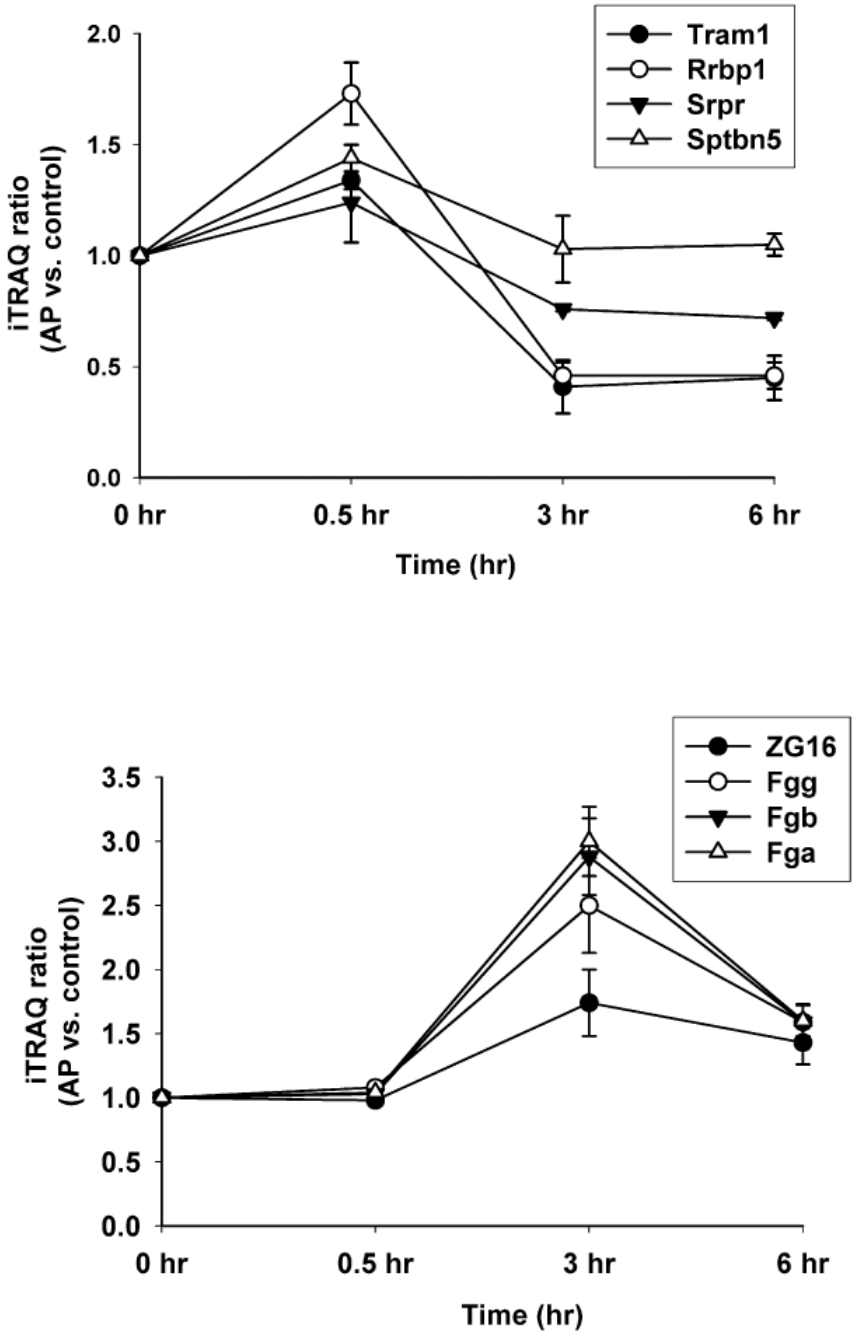

Figure 6. Quantitative proteomics study revealed RER protein changes during AP with different time courses

In the 8-plexed iTRAQ experiment, RER samples from caerulein-induced AP rats were prepared at 0, 0.5, 3 and 6 hours after first injection and then protein abundance at different time points were quantitatively compared. Tram1: translocation associated membrane protein 1; Rrbp1, ribosome binding protein 1; Srpr, Signal recognition particle receptor and Sptbn 5, spectrin, beta, non-erythrocytic 5. Fga, Fgb and Fgg: fibrinogen alpha chain, beta chain and gamma chain; ZG16, zymogen granule membrane protein 16.

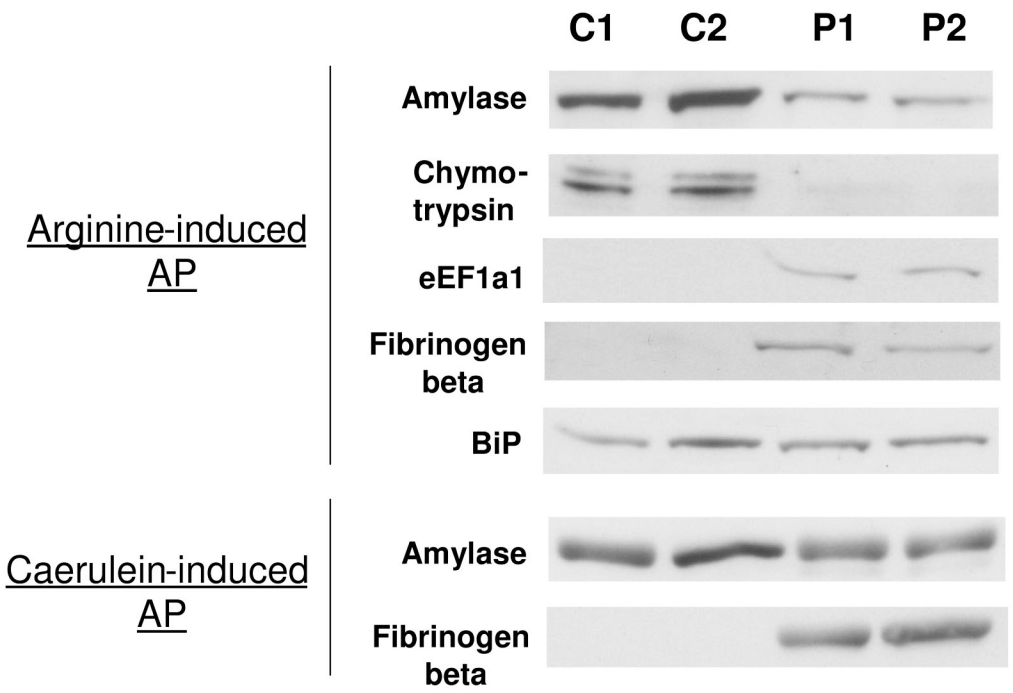

Figure 7. Western blotting confirmation of major RER protein changes detected by the iTRAQ-based quantitative protemics studies

15 μg of RER samples from two control (C1 and C2) and two AP (P1 and P2) were separated on SDS-PAGE gels and analyzed by Western blotting. Antibodies against five major proteins showed significant changes in caeruelin- or arginine-induced AP or in both were used to confirm the iTRAQ ratios.

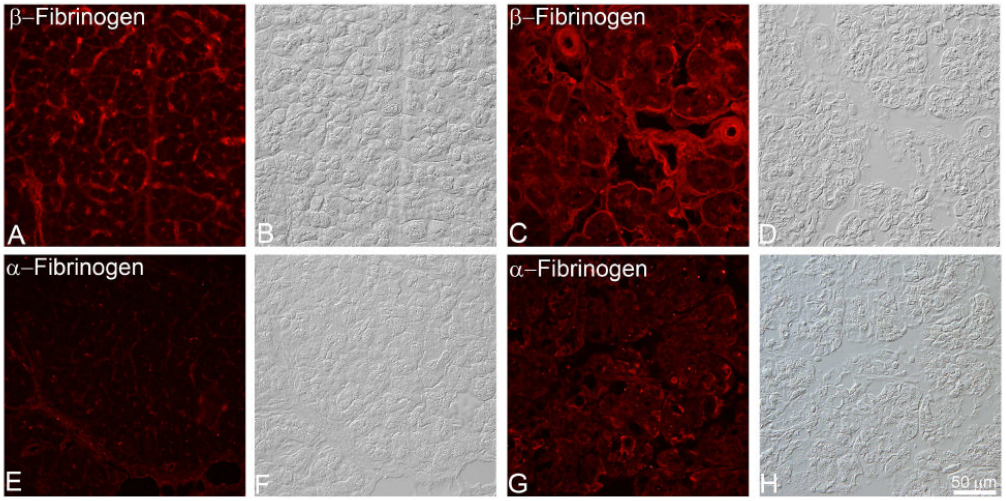

Figure 8. Immunocytochemistry of fibrinogen in normal and acute pancreatitis animals

Localization of beta- and alpha-fibrinogen, with corresponding Nomarski images, in normal rat pancreas (A, B, E, F) and in pancreas after cerulean-induced pancreatitis (C, D, G, H). Beta fibrinogen is localized primarily to extracellular spaces and vasculature in normal pancreas (A). This localization was more pronounced in pancreas with pancreatitis (C) in which disruption of normal morphology, including edema, was readily apparent in Nomarski images (compare B and D). In pancreas from control rats, alpha fibrinogen was localized weakly to extracellular spaces, including vasculature (E), and pancreas morphology (F) was normal, whereas in pancreas from animals with pancreatitis, some acinar cells exhibited cytosolic staining, particularly in areas with damaged cells and edema (H).

J Proteome Res. Author manuscript; available in PMC 2011 February 5.

Table 1

Up- and down-regulated RER proteins in arginine-induced acute pancreatitis rats

			Experiment #1		Experiment #2	
	Gene symbols and protein names	**Function**	**Ratio treatment/control**	**# of peptides**	**Ratio treatment/control**	**# of peptides**
Rnase1	Ribonuclease pancreatic precursor isoform 1	Digestive enzyme	0.26 ± 0.05**	3	0.14 ± 0.08*	3
Cpb1	Carboxypeptidase B1 precursor	Digestive enzyme	0.30 ± 0.07**	4	0.36 ± 0.04**	8
Cpa1	Carboxypeptidase A1 precursor	Digestive enzyme	0.36 ± 0.16	3	0.23 ± 0.05**	11
Pnlip	Pancreatic triacylglycerol lipase precursor	Digestive enzyme	0.39 ± 0.06**	10	0.29 ± 0.05**	11
Ctrb	Chymotrypsinogen B precursor	Digestive enzyme	0.44 ± 0.05**	3	0.24 ± 0.06**	7
Amy2	Pancreatic alpha amylase precursor	Digestive enzyme	0.46 ± 0.04**	24	0.24 ± 0.04**	17
Ctrl	Chymopasin	Digestive enzyme	0.47 ± 0.02**	3	0.24 ± 0.03**	3
Rab7	Ras related protein Rab7a	Small GTPase	0.50 ± 0.00**	1	0.79 ± 0.20	3
Pnliprp1	Pancreatic lipase related protein 1 precursor	Digestive enzyme	0.50 ± 0.02**	4	0.31 ± 0.05**	5
Cel	Bile salt activated lipase precursor	Digestive enzyme	0.53 ± 0.10	3	0.28 ± 0.05**	8
Erp27	Endoplasmic reticulum p27	Chaperone	0.72 ± 0.06*	5	0.48 ± 0.16*	9
Ela3b	Elastase 3B, pancreatic	Digestive enzyme	0.73 ± 0.08	1	0.25 ± 0.03**	3
P4hb	prolyl 4-hydroxylase, beta polypeptide	PDI like	0.80 ± 0.02**	17	0.60 ± 0.08**	40
Hspa5	78 kDa glucose regulated protein precursor (Bip)	Chaperone	0.81 ± 0.03**	26	0.59 ± 0.06**	41
Sel1h	Sel1 (suppressor of lin12) 1 homolog	Signaling	0.93 ± 0.11	4	0.54 ± 0.02*	2
Gnb2l1	Guanine nucleotidebinding protein subunit beta2 like 1	GTPase	1.08 ± 0.17	2	2.03 ± 0.35**	7
C3	Complement C3 precursor (Fragment)	Clotting factor	1.76 ± 0.09*	2		
Tubb4	Tubulin, beta 4	Cytoskeleton	1.98 ± 0.37*	3		
Pabpc4	Poly(A) binding protein, cytoplasmic 4 isoform 1	Protein synthesis	2.5 ± 0.73*	4	2.94 ± 0.55**	8
Tubb5	Tubulin beta5 chain	Cytoskeleton	2.59	1	2.3 ± 0.37**	8

			Experiment #1		Experiment #2	
	Gene symbols and protein names	**Function**	**Ratio treatment/control**	**# of peptides**	**Ratio treatment/control**	**# of peptides**
Tuba4a	Tubulin alpha4A chain	Cytoskeleton	2.69 ± 0.38**	1	3.61 ± 0.27**	3
Eef1a1	Elongation factor 1alpha 1	Protein synthesis	2.98 ± 0.88**	6	2.71 ± 0.45**	8
Vtn	Aa1018 Vitronectin	Inhibition of thrombin	3.01 ± 0.93*	4	2.28 ± 0.90	2
Snd1	Staphylococcal nuclease domain containing protein 1	Transcription coactivator	3.45 ± 0.42**	5	2.93 ± 0.26**	10
Hdlbp	Vigilin (high density lipoprotein binding protein)	lipid transport	3.77 ± 0.00	1	2.80 ± 0.39**	14
Tuba1c	Tubulin alpha1C chain	Cytoskeleton	4.21 ± 0.70*	2	2.31 ± 0.64	2
Fgg	Fibrinogen gamma chain precursor	Clotting factor	4.60 ± 0.93**	11	2.42 ± 0.93	3
Fga	Fibrinogen alpha chain precursor	Clotting factor	5.23 ± 0.79**	12	2.99 ± 0.59**	4
Fgb	Fibrinogen beta chain precursor	Clotting factor	6.55 ± 1.51**	14	2.00 ± 0.54	3
Eif4a1	Eukaryotic translation initiation factor 4A	Protein synthesis	8.71 ± 3.39*	3	5.77 ± 1.39**	8
Ddx3x	Similar to ATPdependent RNA helicase DDX3X	Protein binding			2.84 ± 0.67**	9

Two biological replicate experiments were conducted to compare the abundances of RER proteins from normal and arginine-induced pancreatitis rats using iTRAQ-based quantitative proteomics. RER proteins are listed in the table based on the criteria: in at least one of the two experiments, proteins were detected with ≥ 95% confidence and showed statistically significant changes ($p \leq 0.05$) with a mean ratio of either >1.50 or <0.75. Protein ratios are expressed as Mean ± S.E. and

* represents $p \leq 0.05$ and

** $p \leq 0.01$. Numbers of unique peptides for each protein are also listed in the table.

Table 2

Up- and down-regulated RER proteins in caerulein-induced acute pancreatitis rats

			Experiment #1		Experiment #2	
	Gene symbols and protein names	**Function**	**Ratio Tretament/control**	**# of peptides**	**Ratio Tretament/control**	**# of peptides**
Rrbp1	Ribosomebinding protein 1	Protein synthesis	0.11 ± 0.03**	7	0.46 ± 0.06**	19
Erp27	Endoplasmic reticulum p27	Chaperone	0.60 ± 0.08**	5	0.89 ± 0.01	10
Srpr	Signal recognition particle receptor	Translocon	0.62 ± 0.03*	1	0.72 ± 0.01**	2
Ppib	Peptidylprolyl cistrans isomerase B precursor	Isomerase Digestive	0.64 ± 0.03**	6	0.90 ± 0.03	5
Pnlip	Pancreatic triacylglycerol lipase precursor	enzyme	0.65 ± 0.02**	4	0.83 ± 0.03**	10
Lrrc59	Leucine rich repeat containing protein 59	Protein synthesis	0.65 ± 0.04**	6	0.88 ± 0.04	6
Ssr3	Translocon associated protein subunit gamma	Translocon	0.66 ± 0.03**	1	1.01 ± 0.21	8
Rpn2	Dolichyldiphosphooligosaccharide protein glycosyltransferase 63 kDa subunit precursor	Protein glycosylation	0.69 ± 0.06**	4	1.04 ± 0.02	4
P4hb	prolyl 4-hydroxylase, beta polypeptide	PDI like	0.72 ± 0.02**	26	0.92 ± 0.01	35
Fga	Fibrinogen alpha chain precursor	Clotting factor	5.24 ± 0.83**	16	1.60 ± 0.12**	21
Fgg	Fibrinogen gamma chain precursor	Clotting factor	9.43 ± 2.80**	13	1.59 ± 0.14**	11
Fgb	Fibrinogen beta chain precursor	Clotting factor	9.52 ± 1.84**	24	1.59 ± 0.13**	23

Two seperate biological experiments were conducted to compare the abundances of RER proteins from normal and caerulein-induced pancreatitis rats using iTRAQ-based quantitative proteomics. RER proteins are listed in the table based on the criteria: in at least one of the two experiments, proteins were detected with ≥ 95% confidence and showed statistically significant changes ($p \leq 0.05$) with a mean ratio of either >1.50 or <0.75. Protein ratios are expressed as Mean ± S.E. and

* represents $p \leq 0.05$ and

** $p \leq 0.01$. Numbers of unique peptides for each protein are also listed in the table.